

# **Optimal Design of Gating Systems**

## **by Gradient Search Methods**

Carlos E. Esparza

NEMAK S.A. de C.V.

Libramiento Arco Vial Km. 3.8

García, NL 66000, México

E-mail: *cesparza@nemak.com*

Martha P. Guerrero-Mata

Universidad Autónoma de Nuevo León

Facultad de Ingeniería Mecánica y Eléctrica

Pedro de Alba S/N, Cd. Universitaria,

San Nicolás de los Garza, NL 66450, México

E-mail: *mguerre@gama.fime.uanl.mx*

Roger Z. Ríos-Mercado\*

Universidad Autónoma de Nuevo León

Graduate Program in Systems Engineering

AP 111-F, Cd. Universitaria

San Nicolás de los Garza, NL 66450, México

E-mail: *roger@uanl.mx*

December 2004

Revised April 2005

---

\* Corresponding author

## Abstract

A numerical optimization technique based on gradient-search is applied to obtain an optimal design of a typical gating system used for the gravity process to produce aluminum parts. This represents a novel application of coupling nonlinear optimization techniques with a foundry process simulator, and it is motivated by the fact that a scientifically guided search for better designs based on techniques that take into account the mathematical structure of the problem is preferred to commonly found trial-and-error approaches. The simulator applies the finite volume method and the VOF algorithm for CFD analysis. The direct gradient optimization algorithm, sequential quadratic programming (SQP), was used to solve both 2D and a 3D gating system design problems using two design variables. The results clearly show the effectiveness of the proposed approach for finding high quality castings when compared with current industry practices.

PACS Codes: 82.20.Wt, 83.10.Ji, 81.05.Bx, 02.60.Pn, 02.70.Fj, 07.05.Fb

Keywords: Gating system, computational modeling, design optimization, VOF method, direct gradient optimization.

# 1 Introduction

One of the key elements to make a metal casting of high quality is the design of a good gating system. The gating system refers to those channels through which the metal flows from the ladle to the mold cavity. The use of a good gating system is even more important if a casting is produced by a gravity process. If poor gating techniques are used, invariably, lower casting quality is achieved, because of damage on the molten metal received during the flow through the gating system [1]. It could be even worse, if the molten material is a sensitive metal for receiving damage during the filling, because of dross and slag formation. The aluminum and their casting alloys are considered in this category [2,3,4].

Aluminum alloys are very reactive to oxygen and form an oxide,  $\text{Al}_2\text{O}_3$ . When flow is smooth, this oxide tends to form and remain on the surface of the stream. However, when flow is turbulent, the oxide goes into the molten metal stream and may carry gas or air bubbles with it. The oxides remain on the turbulent flow without flotation, because their densities are similar to aluminum. Then, to avoid damage to the molten aluminum, the gating system must be designed to eliminate the air by avoiding conditions which permit aspiration due to formation of low pressure areas. Keeping the speed of the molten aluminum below of 0.50 m/s [4,5,6] and a smooth stream is equally important. In order to achieve a good gating system design, it is necessary to start following basic principles. Molten metals behave according to fundamental hydraulic principles [2]. Applying those fundamentals to the design of the gating system can be an advantage.

The hydraulic factors that affect the flow of molten metals are: (a) Bernoulli's Theorem, (b) Law of Continuity, (c) Momentum Effects, (d) Frictional Forces, and (e) Reynolds' Number. In the past decades some equations based on empirical relationships have been derived and used to design a gating system [2]. After applying these relationships, a gating system of questionable quality is obtained. Typically modifying the mold geometry by applying trial-and-error approach, a better gating system is obtained. However, this trial-and-error approach costs time and money.

During the 90's a lot of developments of software for simulation had been done for the foundry process [7,8,9]). Some of these programs, Sirrell, Holliday, and Campbell [10,11], Yang, Jolly, and Campbell [12], Jolly et al. [13], Ha et al. [14], and Schuhmann et al. [15], were able to simulate the behavior of the molten metal close to reality, as they studied the behavior of the molten aluminum during the filling of different gating systems by optical means, and correlated the measurements to

obtain the behavior by some simulators. By the end of the 90's the trial-and-error approach practices moved away from the real mold to the virtual one, obtaining a better final design, but still not the optimum design.

A logical step to achieve an optimum gating design and overcome the expensive trial-and-error approaches is to develop an automatic optimization process. Essentially, this involves the coupling of a process simulator that solves the flow problem with an optimization technique, which iteratively finds a search direction that guarantees a better design is obtained in every step. The procedure terminates with a design that is locally optimal with respect to the design variables

The purpose of this paper is to demonstrate how the application of numerical optimization techniques can be used to search effectively for an optimum gating system design. This approach is evidently superior to typical trial-and-error approaches commonly followed in the industrial environment. The rest of the paper is organized as follows. In Section 2, we briefly sketch the closest previous work. The flow governing equations are established in Section 3. This is followed by a description of a typical gating design system in Section 4. In Section 5, the overall solution methodology is presented. In Chapters 6 and 7, we present our computational experience and discussion of the results, respectively. We wrap up this work with our conclusions in Section 8.

## 2 Related Work

To the best of our knowledge, there have been very few attempts to use optimization techniques for addressing the problem discussed here. The first published work showing an effort to apply a numerical optimization methodology to optimize a gating system is due to Bradley and Heinemann [16] in 1993. They used simple hydraulic models to simulate the optimization of the gating during the filling of molds. Apparently this work has never been implemented [17].

Other published work related to gating optimization was carried out by McDavid and Dantzig [17,18] in 1997. Their entire simulation phase was 2-dimensional (in terms of the mold geometry). Their approach also used a mathematical development addressing the design sensitivity. The simulator used was FIDAP, a FEM based program for flow simulation. No velocity constraints were imposed at the ingates.

### 3 Flow Governing Equations

#### 3.1 Mathematical model

The governing equations that describe the physical and metallurgical phenomenon can be represented in a generic form as follows [19]:

$$\frac{\partial}{\partial t}(\rho\phi) + \frac{\partial}{\partial x_j}(\rho U_j \phi) = \frac{\partial}{\partial x_j} \left( \Gamma^\phi \frac{\partial \phi}{\partial x_j} \right) + S^\phi \quad (1)$$

Governing differential equations of continuity, momentum, energy and volume of fluid (VOF), can be obtained depending of the values taken by the governing variable  $\phi$ , the diffusion coefficient  $\Gamma^\phi$  and the internal energy source term  $S^\phi$ . Table I summarizes each of the coefficients to be replace on equation (1) in order to obtain any of the governing equations.

Thereby, as an example, if the values of  $\phi$ ,  $\Gamma^\phi$  y  $S^\phi$  from the above table are substituted on equation (1) the Volume of Fluid equation, VOF, is obtained as:

$$\frac{\partial F}{\partial t} + v_x \frac{\partial v_x}{\partial x} + v_y \frac{\partial v_y}{\partial y} + v_z \frac{\partial v_z}{\partial z} = 0 \quad (2)$$

For void or empty elements the F value is 0.0, for complete filled elements the F value is 1.0, and for the partial filled elements the F value varies from 0.0 to 1.0. This fraction represents the free surface of the flow stream.

#### 3.2 Solving the Governing Equations

To solve the governing equations that represent the mold-filling phenomenon, numerical techniques were used. The commercial program FLOW3D applies the generic method SOLA-VOF [20]. This method has been very popular over the last few years for its ability to track free surfaces. To simulate the flow of molten metal, the model has been extensively modified to include heat transfer and solidification effects.

## 4 A Typical Gating System Design

In 1995, Sirrell, Holliday and Campbell [10,11] conducted a research benchmark among nine different filling simulation programs available at that time. Their study started designing a typical gating system (shown in Figure 1). A key element for the experiment consisted of filming the filling of the system with an X-Ray video camera. The gating system design was simple. The CAD capabilities of the different programs were not a target to be measured during the experiment, but the tracking of the free surface and the behavior of the flow. Choosing a sprue height of more of 300 mm had the intention to produce enough turbulence on the molten metal as it was falling. Because of ease to any of the participants for funding the thermo physical data, pure aluminum was selected as the poured material. A comparison between the experimental results and all the simulation results presented by each of the nine teams was done.

Flow3D [21], was one of the programs that better predicted the qualitative behavior of the movement of the molten aluminum. To develop the present work, Flow3D was chosen to simulate the same gating system. However the target was to optimize the design to eliminate the aspiration of air on the system before the melt reached the ingate.

## 5 Description of Proposed Gating System Optimization Methodology

### 5.1 Numerical Optimization Techniques

Traditionally numerical optimization has been developed within the operations research community [22]. The basic idea behind a numerical optimization based on gradient-search method is to search for an optimal solution  $X$  (set of decision variables) within a feasible search space (set of decision variables that satisfy all technological constraints) that would optimize the value of an objective function  $F(X)$ . This objective function must measure the cost or performance of the given problem as a function of the decision variables. The theory supporting these methods guarantees that this search is carried out iteratively in such a way that a better solution is reached at every iteration. The process continues until a stopping criteria is satisfied. This stopping criteria could be (a) local-optimality conditions, or (b) time/iteration limit reached. In the case of study, the decision variables correspond to the design variables.

## 5.2 Choosing the Optimization Method

For this particular application, one key issue was to achieve the coupling of a gradient-based optimization algorithm (that would guide the search for an optimal design) with a program that simulates the fluid flow for a given design. The starting point was the solution of the flow problem on an initial design  $X$  (or initial solution), to determine the performance of the given design. Then, this information from the simulator was used within a numerical optimization framework to determine a search-direction for  $X$ , iteratively.

In a preliminary study with different optimization methods [23], it was found that a Sequential Quadratic Programming (SQP) method exhibited better performance. Therefore for the present work, VisualDOC [24], an optimization program that allows both implementation of SQP, and coupling to almost any CAE or CFD programs (including Flow3D) to simulate different kind of flow processes, was used. Figure 2 shows the overall solution procedure, and the interaction between both methods.

## 5.3 Optimization Model Description

For the present problem, the following formulation was used.

*Design Variables* (see Figure 3):

$ZL$   $\equiv$  Runner depth (cm)

$CX$   $\equiv$  Slope on the tail

*Indices/Sets*:

$i \in I$   $\equiv$  Discretization elements / cells of the runner.

$j \in J$   $\equiv$  Discretization elements / cells of the ingate.

*Parameters*:

$ZL_l$   $\equiv$  Lower limit of the runner depth (cm)

$ZL_u$   $\equiv$  Upper limit of the runner depth (cm)

$CX_l$   $\equiv$  Lower limit of slope on the tail

$CX_u$   $\equiv$  Upper limit of slope on the tail

*Auxiliary Variables:*

$tc_i \equiv$  Filling time of element  $i$  of the runner;  $i \in I$  (sec.)

$te_j \equiv$  Filling time of element  $j$  of the ingate;  $j \in J$  (sec.)

$Vx_j \equiv x$ -component of the aluminum velocity in the  $j$ -th ingate element;  $j \in J$  (cm/s)

$Vy_j \equiv y$ -component of the aluminum velocity in the  $j$ -th ingate element;  $j \in J$  (cm/s)

$Vz_j \equiv z$ - component of the aluminum velocity in the  $j$ -th ingate element;  $j \in J$  (cm/s)

$V_j \equiv$  Objective function that represents the aluminum velocity at the  $j$ -th ingate element,

$$j \in J .$$

*Formulation*

$$\text{Minimize } V_j(ZL, CX) = \sqrt{Vx_j^2 + Vy_j^2 + Vz_j^2} \quad (3)$$

subject to:

$$tc_i \leq te_j \quad i \in I, j \in J \quad (4)$$

$$ZL_l \leq ZL \leq ZL_u \quad (5)$$

$$CX_l \leq CX \leq CX_u \quad (6)$$

Constraints (4) indicate that the filling time for the runner elements must not exceed the filling time for the ingate elements. This constraint assures that the runner is filled out before the ingate, i.e., preventing the formation of air bubbles that would cause a product with low quality. Constraints (5)-(6) represent the physical limits on the design variables. Figure 3 shows a physical layout of the mold geometry.

## 6 Computational Experiments

### 6.1 Preliminary Study

As stated in Section 5.1, the SQP algorithm was chosen as the core of our optimization engine. To understand the influence of the design variables and other parameters that affect the gating system design performance, two numerical experiments were carried out. In the first experiment, our objective was to evaluate the method performance when using different values of the step size (SS) parameter, or signal factor, and starting solution values for both design variables (ZL and CX). It is well known from nonlinear optimization that the method's performance may be affected by the choice of the starting solution and the value of SS, so this motivates our experiment. This first DOE was run using a coarse mesh representation of the selected gating system. Although results are much more accurate when using finer mesh sizes, what we expect to gain here is to reduce computational effort so we can make more runs and find out relatively quickly the effects of SS.

For our experimental design (DOE), a Taguchi L9 array was used. The complete set of analysis included 27 executions (one replication per cell), using 3 factors at 3 levels each ( $3^3 = 27$ ). The values used for the starting solution values of the two design variables and the step size parameter are shown in Table II. The levels 1, 2, and 3 of SS shown in the table correspond to  $1 \times 10^{-2}$ ,  $1 \times 10^{-5}$ , and  $1 \times 10^{-7}$ , respectively. As previously stated, the method aims at finding values of the design variables that would minimize the velocity of the aluminum at the ingate. Results are shown in Section 7.

### 6.2 Application on a Real 3D Gating System Design

After performing the first experiment, one of the key conclusions was that the best value for SS was between  $1 \times 10^{-2}$  and  $1 \times 10^{-5}$ . So, our second experiment aims at evaluating the method performance for different starting values of the design variables on a real 3D gating system design. This time, we use a finer mesh to improve accuracy and a fixed value of SS ( $1 \times 10^{-4}$ ). A Taguchi L9 array was used, 2 design factors with 3 levels ( $3^2 = 9$ ). Starting values of the design variables are shown in Table III. Again, the analysis and results are shown in the following section. As expected, the computational time needed to complete each analysis increased significantly.

## 7 Results and Discussion

### 7.1 Flow3D Simulation Results vs. Experimental Results

A correlation study was done to justify the use of Flow3D as the simulator. Results obtained by Sirrell, Holliday, and Campbell [10] at 0.75 seconds after the start of the filling of the gating system are shown in Figure 4(a), where the set of pictures indicate results of three different experiments at the same time. Figure 4(b) show the Flow3D results at three different times. The simulation results at 0.9 sec indicate a high correlation with the experimental results showed (at 0.75 sec), so the same behavior was found with a delay time of around 0.15 sec. The use of Flow3D to simulate the gravity process is found acceptable as it captures the turbulent behavior of the molten metal including position of the free surface with high accuracy.

### 7.2 Results and Analysis of Experiment 1

Results obtained from the DOE of Table III are analyzed with Minitab [25] and shown in Figures 5 and 6. Figure 5 shows the influence the initial values of the design variables ZL and CX and the signal factor SS have on the quality of the final solution. As can be seen, the choice of the initial value for the runner depth, ZL, seems to have a higher effect. More specifically, high starting values for ZL gave the best results. For CX, the best results were observed when its initial value started at a high value. The influence of the signal factor, SS, seems to have little effect on the objective function. However, lower values for SS ( $1 \times 10^{-2}$  or  $1 \times 10^{-5}$ ) produced better results.

Figure 6 shows the interaction between the three factors. The use of the two higher values of the starting value of ZL helps to obtain a better design that minimizes the aluminum velocity at the ingate regardless the value of SS or the initial value of CX. Similar conclusion can be drawn when the starting value of CX is 1.5, no matter what values are used with the other two factors.

Finally, it can be concluded that using an initial value of ZL between 10.25 cm and 10.75 cm, an initial CX value of 1.5, which is equivalent to a  $60^\circ$  angle of the runner tail, and SS equal to  $1 \times 10^{-5}$  the best gating system design is achieved. Similar statements can be concluded from Figures 7 and 8.

Figure 9 is a 3D plot of the aluminum velocity at the ingate as a function of the final values of the design factors, the optimal values of ZL and CX. The optimized gating system includes a ZL value between 10 and 10.9 and a CX value higher than 1.0. With that design an expected velocity between 25 and 30 cm/sec is obtained. We recall that this first set of results was obtained using a coarse mesh, which can be simulated relatively fast, providing us with insight and understanding of the influence of the design factor. A more realistic study was carried out using a finer mesh.

### 7.3 Results and Analysis of Experiment 2

In Figure 10 the influence of the selection of the initial values of the design variables ZL and CX is shown. Both factors (ZL and CX) behave in a similar fashion. Starting ZL in a low value and CX in a high value yield better performance. The interaction between the two initial values of the design variables is shown in Figure 11. The use of the lower value of ZL, 9.5, helps to obtain a better design that minimizes the aluminum velocity at the ingate, no matter what value of CX is used. Similarly, setting a value of 1.5 for CX, no matter what ZL value is used, delivers a better design. Figure 12 shows a 3D plot of the aluminum velocity at the ingate as a function of the first values of the design variables. It can be seen that at the lower and upper values of both design variables, resulting in four combinations (9.5, 0.3; 9.5, 1.5; 10.9, 0.3; and 10.9, 1.5), an optimal gating system design is better achieved, avoiding the use of other sets of combinations.

Figure 13 is a 3D plot of the aluminum velocity at the ingate as a function of the final values of the design variables, the optimal values of ZL and CX. The optimized gating system includes a ZL value between 10.79 and 10.91 and a CX value higher than 1.5. With these values, velocity lies between 35.6 and 37.6 cm/sec. These results have been obtained with a finer mesh giving a more realistic result.

A comparison between the results obtained using the original runner vs. the optimum design was carried out using the foundry criteria. Figures 14 to 19 show different results from the original and the optimal runner. Figure 14 shows the original gating design when the ingate is activated, the aluminum goes into the mold cavity, and some air is trapped in the runner. Figure 15 shows the optimized gating design when the ingate is activated, the aluminum goes into the mold cavity, and there is not air trapped in the runner. This happened at filling time of 0.55 sec.

Figure 16 shows the original gating design and three particle tracers, A, B, and C. The tracers show the pathway that each of these particles follows within the aluminum stream movement. Tracer of particle C shows that some aluminum circulates back into the main runner as the system continues to fill up. Figure 17 shows the optimized gating design and three particle tracers, A, B, and C. The tracers show that the liquid moves forward progressively while the system continues to fill up (without returning to the main runner).

Figure 18 shows the plot of the filling time of each of the control volumes or cells of the original gating design. The filling time of some cells of the main runner is bigger than the time needed to fill the ingate cells. Figure 19 shows the plot of the filling time of each of the control volumes or cells of the optimized gating design. The filling time of all the cells of the main runner is lower than the time needed to fill the ingate cells.

This summarizes how the optimized gating system permits to have aluminum into the mold cavity without trapped air on the main runner or metal coming back to it, improving the original design and showing also the advantages of using the optimization techniques.

## 8 Conclusions

In this work we have presented a methodology for obtaining a gating system design of good quality. To the best of our knowledge, this is the first time an optimization 3D gating system design has been performed, and it is also the first time this has been carried out using FDM CFD programs besides FEM codes.

Two design variables (runner depth, ZL, and runner tail slope, CX) were chosen as decision variables within an optimization phase. In addition, a mathematical nonlinear optimization model was developed with the aim of minimizing the aluminum velocity subject to constraints which ensure there was no trapped air in the main runner when the metal entered the mold cavity via the ingate. The optimization procedure was coupled with a casting process simulator.

Our numerical experiments show the effectiveness of the proposed approach. Our procedure was able to find designs of a better quality than that of current practices. In addition, it was observed that starting the optimization scheme with low values of the runner depth and high values of the runner tail slope yield better designs.

For future work, it would be interesting to study the problem incorporating more design variables. This will of course mean more computational effort, but if this results in even better designs the effort can be worthwhile. Another possibility could be to evaluate different objective functions within the optimization algorithm such as, minimize the bouncing of the molten aluminum moving from one direction to other within the main runner, while keeping restrictions of the ingate velocity below 50 cm/s.

This is a promising approach and a good illustration of how a complex problem can be efficiently tackled by combining the expertise of a concrete engineering application and optimization techniques. We hope this will stimulate further work in this area.

*Acknowledgements:* We would like to thank the full support of NEMAK, S.A. de C.V., Vanderplaats R&D, Inc., and Flow Science, Inc. We are also grateful with the anonymous referees for their helpful comments, which improved the presentation of the paper.

## References

- [1] J. Campbell, *Castings*, Butterworth-Heinemann, London, 1991.
- [2] J.M. Svoboda, Basics principles of gating & risering, American Foundry Men's Society Cast Metals Institute AFS-CMI (1995).
- [3] J. Campbell, Invisible macrodefects in castings, *Journal de Physique IV*, 3 (1993) 861-872.
- [4] J. Runyoro, S.M.A. Bouterabi, J. Campbell, Critical gate velocities for film-forming castings alloys: A basis for process specification, *Transactions of the AFS* (1992) 92-37.
- [5] N.R. Green, J. Campbell, Influence of oxide film filling defects on the strength of Al-7Si-Mg alloy castings, *Transactions of the AFS*, 102 (1994) 341-347.
- [6] J. Campbell, The ten castings rules guidelines for the reliable production of reliable castings: A draft process specification," *Materials Solutions Conference on Aluminum Casting Technology*, Chicago, 1998.
- [7] M. Cross, Casting simulation: Hardware developments, software algorithms and modern developments, Keynote, *Modeling of Casting, Welding and Advanced Solidification Processes (MCWASP IX)*, Aachen, Germany, 2000.
- [8] J. Campbell, Solidification modeling: Current limitations and future potential, *Material Science and Technology*, 2 (1991) 45-52.

- [9] J. Campbell, Review of computer simulation versus casting reality, in: M. Cross, J. Campbell (Editors), *Modeling of Casting, Welding and Advanced Solidification Processes (MCWASP VII)*, London, 1995, pp. 907-913.
- [10] B. Sirrell, M. Holliday, J. Campbell, The benchmark test 1995, in: M. Cross, J. Campbell (Editors), *Modeling of Casting, Welding and Advanced Solidification Processes (MCWASP VII)*, London, 1995, pp. 915-933.
- [11] B. Sirrell, M. Holliday, J. Campbell, Benchmark testing the flow and solidification modeling of Al castings, *Journal of Materials*, 48 (1996) 20-23.
- [12] X. Yang, M. Jolly, J. Campbell, Reduction of surface turbulence during filling of sand castings using a vortex-flow runner, in: *Modeling of Casting, Welding and Advanced Solidification Processes (MCWASP IX)*, Aachen, Germany, 2000, pp. 420-427.
- [13] M.R. Jolly, H.S.H. Lo, M. Turan, J. Campbell, Use of simulation tools in the practical development of a method for manufacture of cast iron camshafts, in: *Modeling of Casting, Welding and Advanced Solidification Processes (MCWASP IX)*, Aachen, Germany, 2000, pp. 311-318.
- [14] J. Ha, R. Schuhmann, V. Alguine, P. Cleary, T. Nguyen, Real-time X-ray imaging and numerical simulation of die filling in gravity die casting, in: *Modeling of Casting, Welding and Advanced Solidification Processes (MCWASP IX)*, Aachen, Germany, 2000, pp. 151-158.
- [15] R. Schuhmann, J. Carrig, T. Nguyen, A. Dahle, Comparison of water analogue modelling and numerical simulation using real-time X-ray flow data in gravity die casting, paper 22, CRC for Cast Metals Manufacturing (CAST), Australia, 1994.
- [16] F. Bradley, S. Heinemann, A hydraulics-based optimization methodology for gating design, *Applied Mathematical Modelling*, 17 (1993) 406–414.
- [17] R.M. McDavid, J.A. Dantzig, Design sensitivity and finite element analysis of free surface flows with application to optimal design of casting rigging systems, *International Journal for Numerical Methods in Fluids*, 28 (1998).
- [18] R.M. McDavid, J.A. Dantzig, Experimental and numerical investigation of mold filling, in: *Modeling of Casting, Welding and Advanced Solidification Processes (MCWASP VIII)*, Chicago, 1998, pp. 59-66.
- [19] F. Bonollo, S. Odorizzi, *Numerical Simulation of Foundry Processes*, Servizi Grafici Editoriali, Padova, Italy, 2001.
- [20] C.W. Hirt, B.D. Nichols, Volume of fluid (VOF) method for the dynamics of free boundaries, *Journal of Computational Physics*, 39 (1981) 201-225.

- [21] M.R. Barkhudarov, C.W. Hirt, Casting simulation: Mold filling and solidification: Benchmark calculations using FLOW-3D, in: M. Cross, J. Campbell (Editors), Modeling of Casting, Welding and Advanced Solidification Processes (MCWASP VII), London, 1995, pp. 935-946.
- [22] G.N. Vanderplaats, Numerical Optimization Techniques for Engineering Design: With Applications, McGraw-Hill, New York, 1984.
- [23] C.E. Esparza-Garcés, R.Z. Ríos-Mercado, M.P. Guerrero-Mata, Evaluando la calidad de técnicas de optimización para un problema de diseño de sistemas de alimentación por gravedad, in Proceedings of the 11th International Technical Panel of Aluminum Processing and Exposition, Cancún, Mexico, 2003 (in Spanish).
- [24] V. Balabanov, D. Ghosh, G. Vanderplaats, VisualDOC: A software system for general-purpose integration and design optimization, 9th AIAA/ISSMO Symposium on Multidisciplinary Analysis and Optimization, Atlanta, 2002.
- [25] Minitab Inc., MINITAB User's Guide 2: Data Analysis and Quality Tools, Release 13 for Windows, State College, PA, 2003.

Equation Name	$\phi$	$\Gamma^\phi$	$S^\phi$
Continuity	1	0	0
Momentum	$u_i$	$\mu$	$-\frac{\partial P}{\partial t} + \rho g_i + S_i^\mu + S_i^d + X_i$
Energy	$T$	$\frac{k}{C_p}$	$\frac{1}{C_p} \left( \mu \Phi_T + L \frac{\partial f_s}{\partial t} + S_T \right)$
Volume of Fluid (VOF)	$\frac{f}{\rho}$	0	0

Table I. Governing equations' coefficients.

Analysis	ZL	CX	SS
1	9.5	0.3	1
2	9.5	0.3	2
3	9.5	0.3	3
4	9.5	0.9	1
5	9.5	0.9	2
6	9.5	0.9	3
7	9.5	1.5	1
8	9.5	1.5	2
9	9.5	1.5	3
10	10.25	0.3	1
11	10.25	0.3	2
12	10.25	0.3	3
13	10.25	0.9	1
14	10.25	0.9	2
15	10.25	0.9	3
16	10.25	1.5	1
17	10.25	1.5	2
18	10.25	1.5	3
19	10.8	0.3	1
20	10.8	0.3	2
21	10.8	0.3	3
22	10.8	0.9	1
23	10.8	0.9	2
24	10.8	0.9	3
25	10.8	1.5	1
26	10.8	1.5	2
27	10.8	1.5	3

Table II. Taguchi L9 DOE array used in experiment 1.

<b>ANALYSIS No.</b>	<b>ZL</b>	<b>CX</b>
1	9.5	0.3
2	9.5	0.9
3	9.5	1.5
4	10.25	0.3
5	10.25	0.9
6	10.25	1.5
7	10.8	0.3
8	10.8	0.9
9	10.8	1.5

Table III. Taguchi L9 DOE array used in experiment 2.

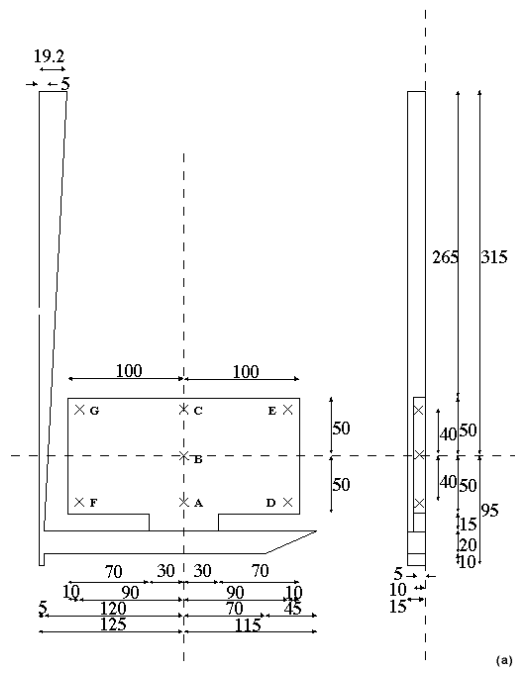


Figure 1. Drawing of the gating system studied by Sirrell, Holliday, and Campbell<sup>[11]</sup>, units, mm.

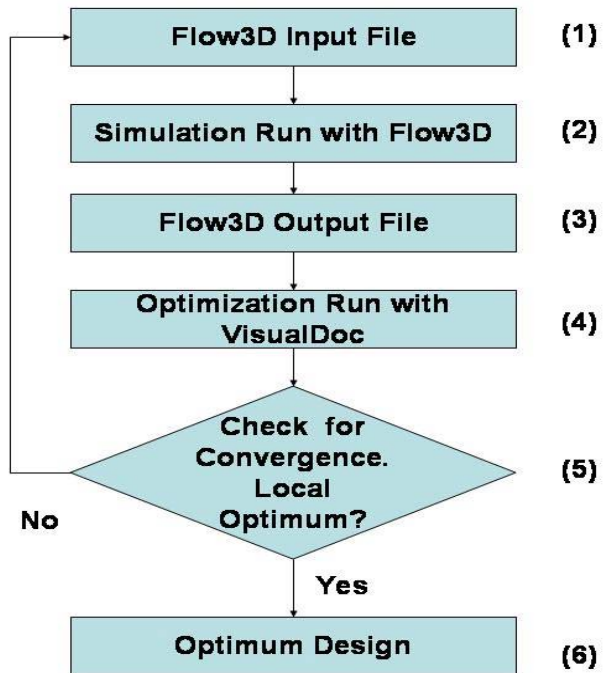


Figure 2. Flow-chart of the overall optimization process.

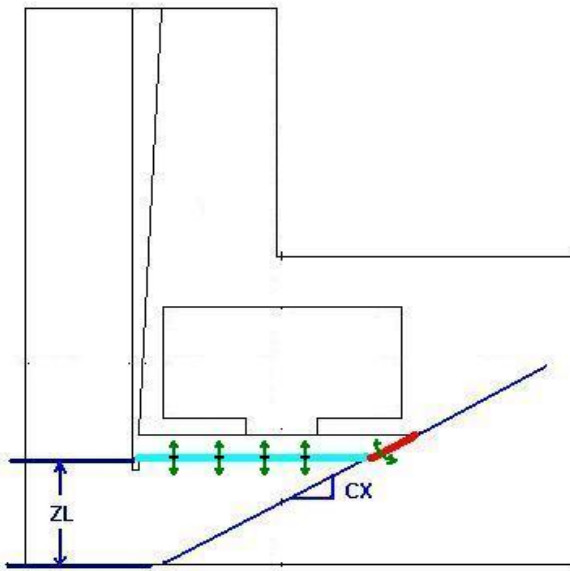


Figure 3. Design variables representation. Runner Depth, ZL, and Runner Tail Slope, CX.

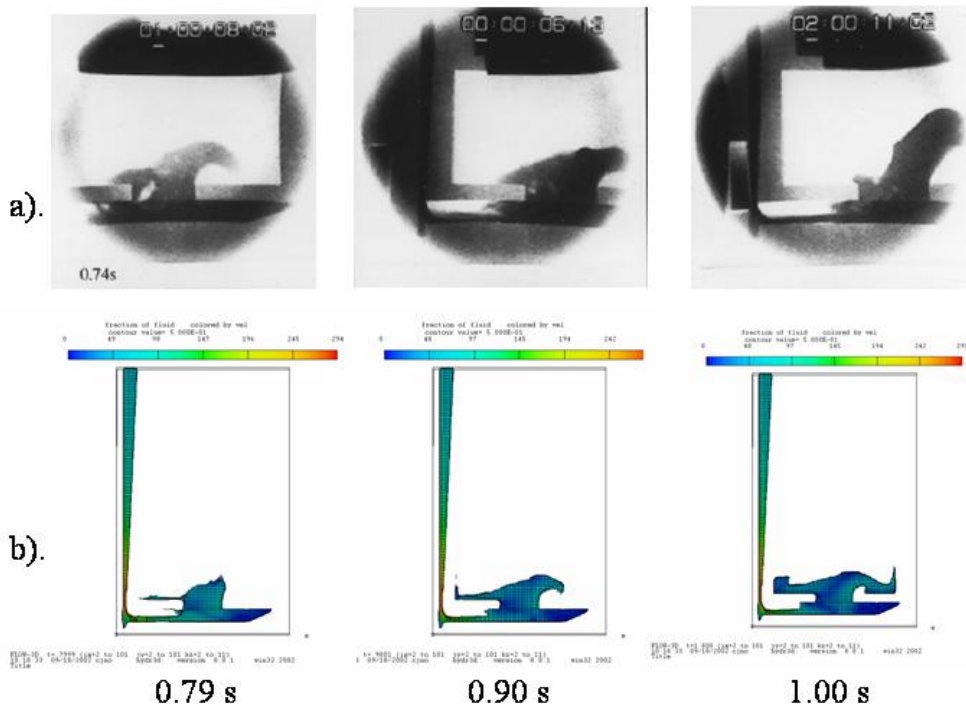


Figure 4. a). Experiment results at 0.75 s.<sup>[1]</sup> and b). Flow3D results at 3 times, 0.79, 0.90 and 1.00 s.

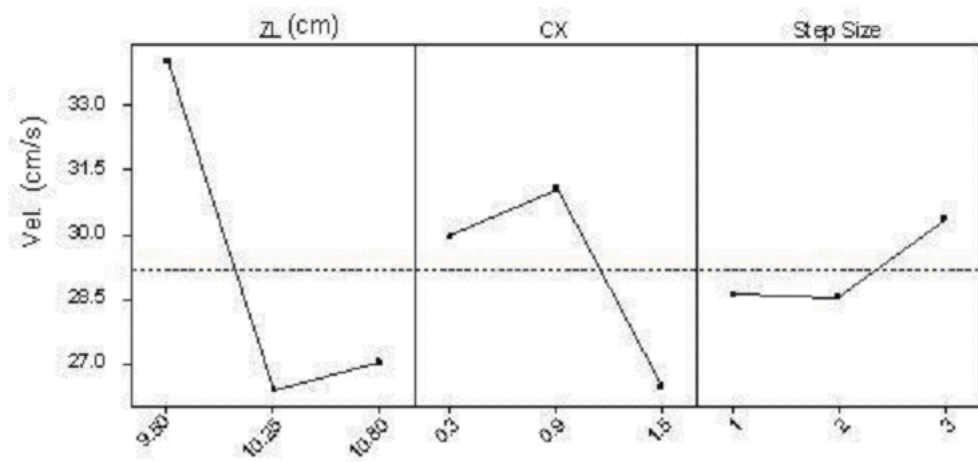


Figure 5. Effect of design variables and signal factor in the objective function.

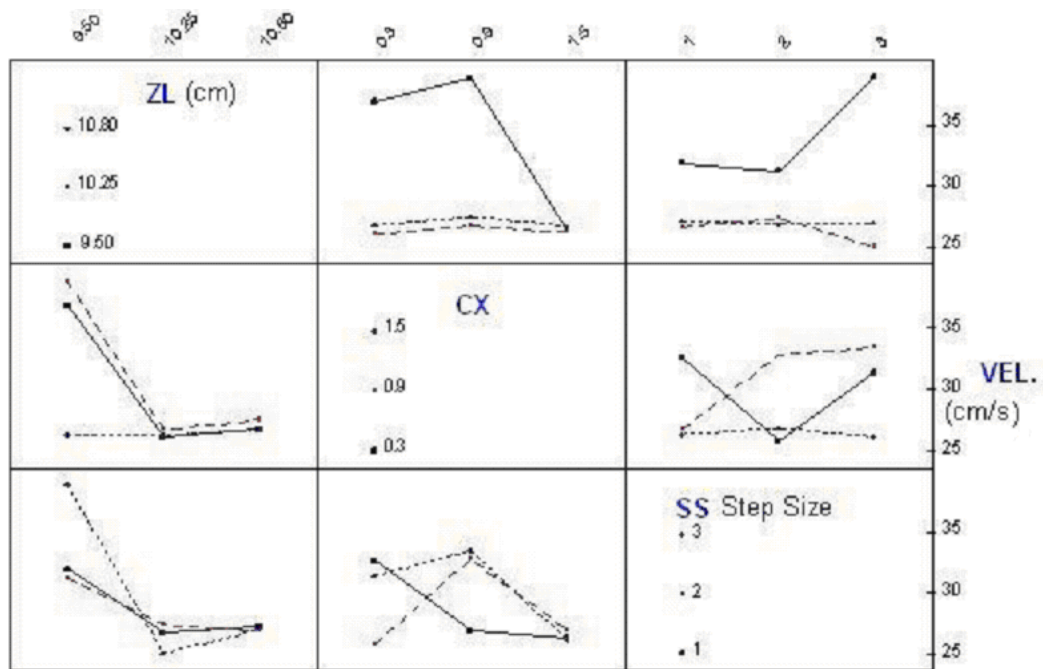


Figure 6. Interaction among design variables and signal factor.

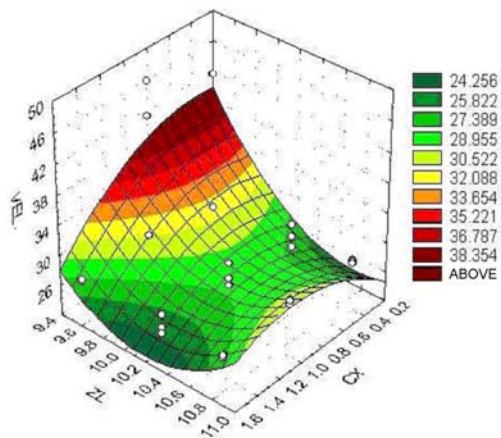


Figure 7. Interaction between the initial values of the design variables ZL and CX to minimize the aluminum velocity at the ingate.

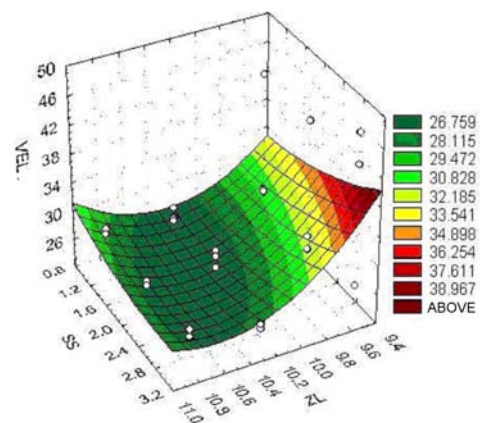


Figure 8. Interaction between the initial values of the design variable ZL and the signal factor SS to minimize the aluminum velocity at the ingate.

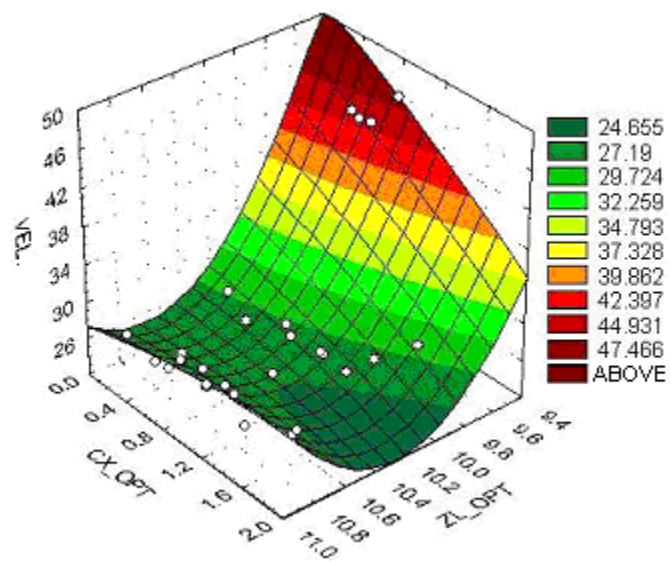


Figure 9. Aluminum velocity at the ingate as a function of the final values of the design factors ZL\_Opt and CX\_Opt.

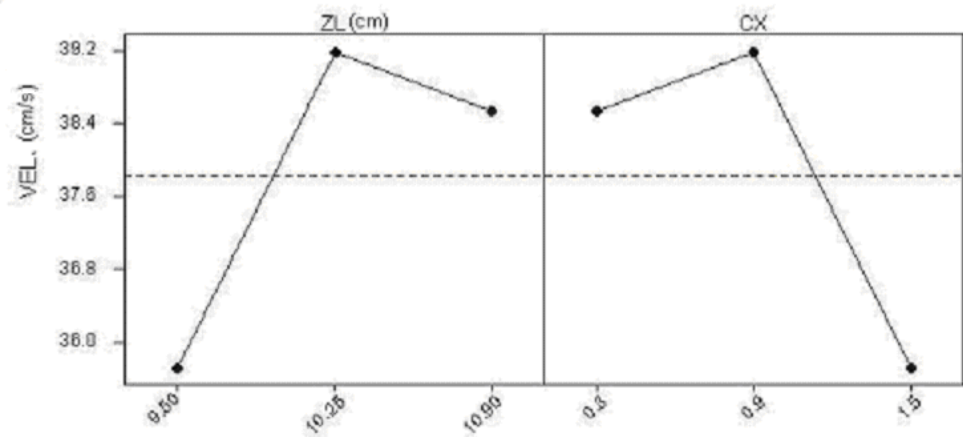


Figure 10. Effect of design variables in the objective function.

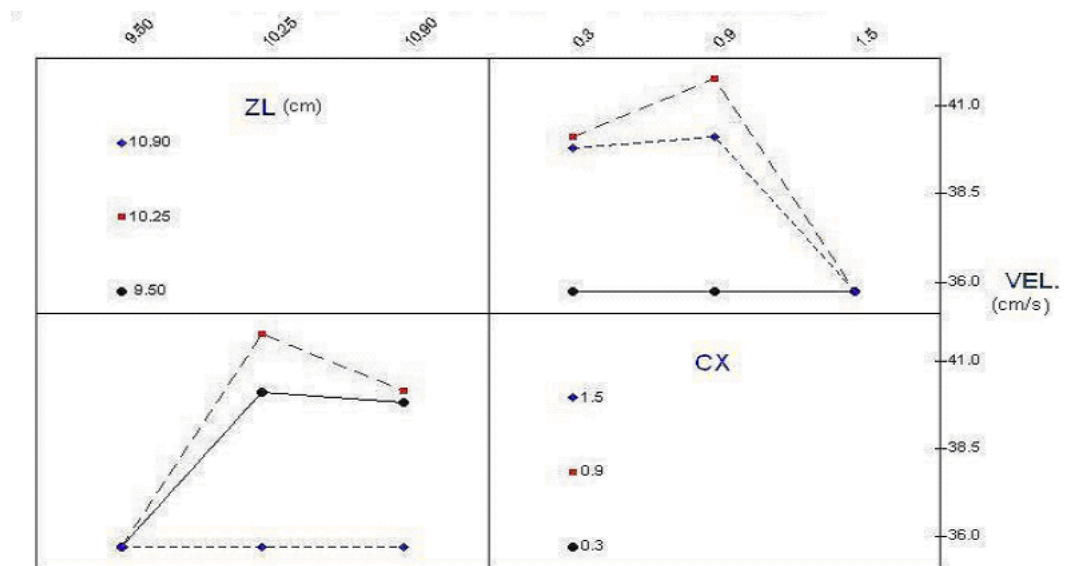


Figure 11. Interaction between the design variables.

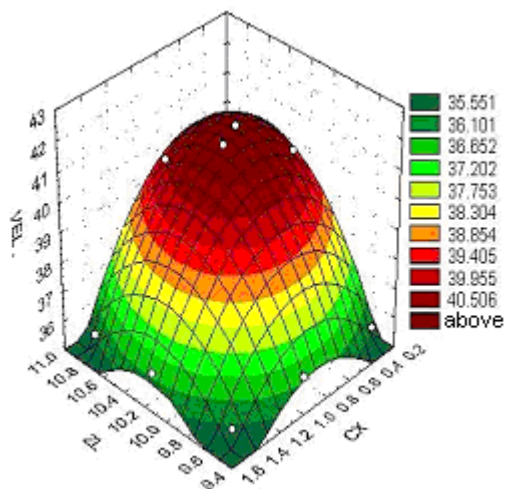


Figure 12. Interaction between the initial values of the design variables ZL and CX to minimize the aluminum velocity at the ingate.

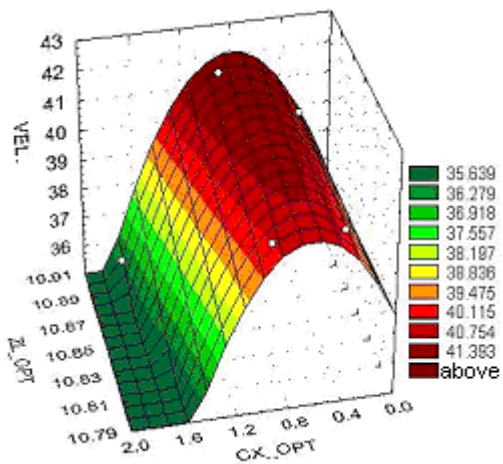


Figure 13. Final values of design variables ZL\_Opt. and CX\_Opt. and their influence to minimize the aluminum velocity at the ingate.

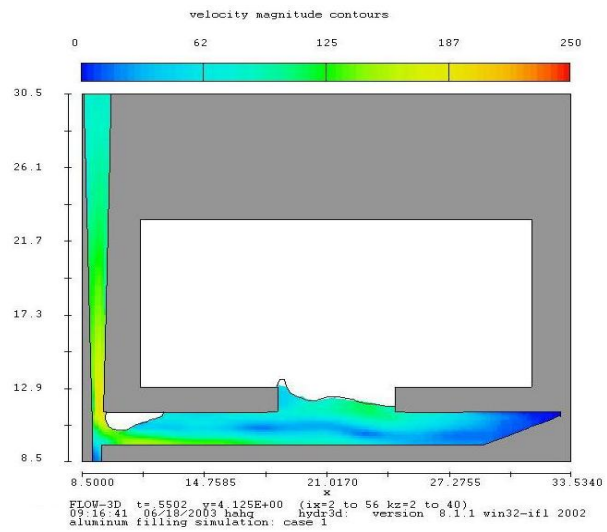


Figure 14. Aluminum velocity in the original gating design when the ingate is activated. Filling time of 0.55 sec.

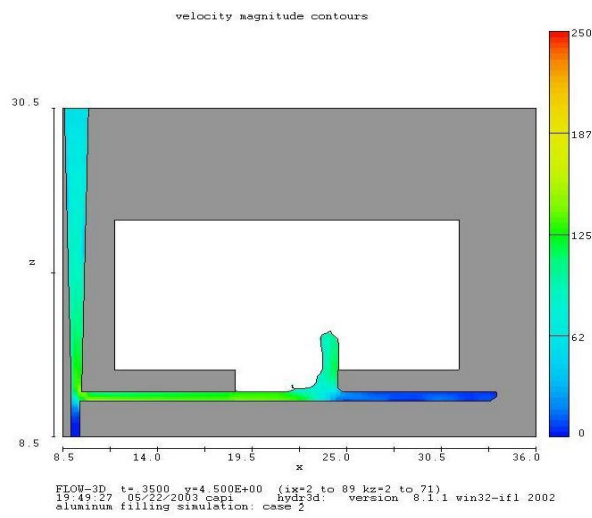


Figure 15. Aluminum velocity in the optimized gating design when the ingate is activated. Filling time of 0.35 sec.

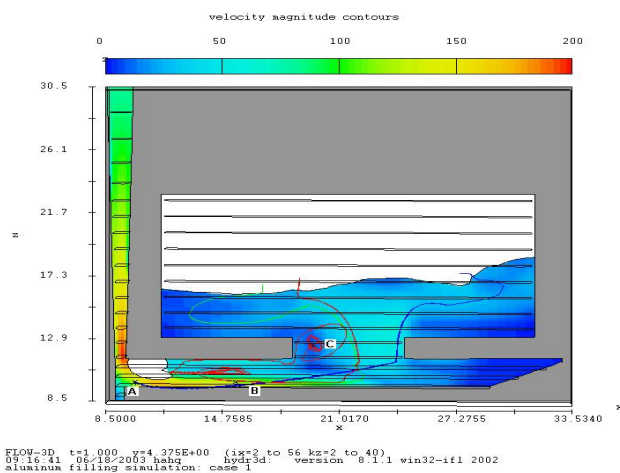


Figure 16. Three tracers of particles, A, B and C displayed with aluminum velocity results obtained using the original gating design at filling time of 1sec.

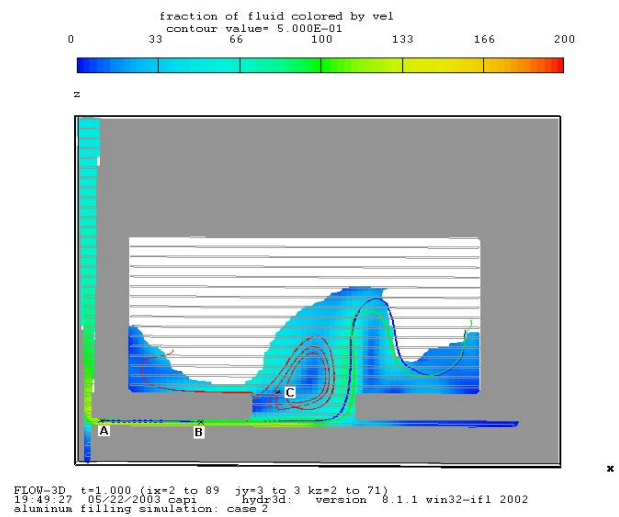


Figure 17. Three tracers of particles, A, B and C displayed with aluminum velocity results obtained using the optimized gating design at filling time of 1 sec.

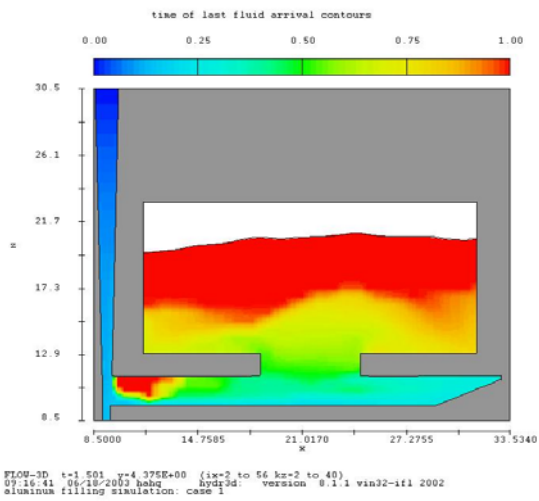


Figure 18. Filling time of each cell or control volume in the original runner.

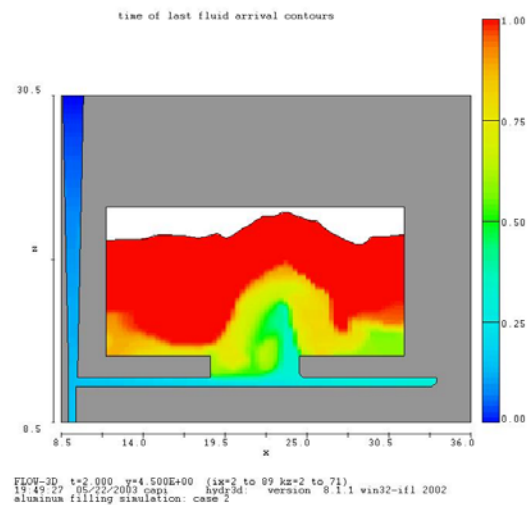


Figure 19. Filling time of each cell or control volume in the optimized runner.